

# Determination of thermoelastic stress wave propagation in nanocomposite sandwich plates reinforced by clusters of CNTs

Babak Safaei, Rasool Moradi-Dastjerdi, Zhaoye Qin, Kamran Behdinan, Fulei Chu

**Version** Post-print/accepted manuscript

**Citation (published version)** Safaei, B., Moradi-Dastjerdi, R., Qin, Z., Behdinan, K., & Chu, F. (2019). Determination of thermoelastic stress wave propagation in nanocomposite sandwich plates reinforced by clusters of carbon nanotubes. *Journal of Sandwich Structures & Materials*. <https://doi.org/10.1177/1099636219848282>.

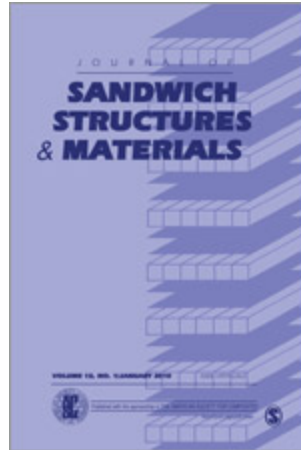
**Copyright/ License** Copyright © 2019 (Sage Publications).

## How to cite TSpace items

Always cite the published version, so the author(s) will receive recognition through services that track citation counts, e.g. Scopus. If you need to cite the page number of the **author manuscript from TSpace** because you cannot access the published version, then cite the TSpace version **in addition to** the published version using the permanent URI (handle) found on the record page.

This article was made openly accessible by U of T Faculty.  
Please [tell us](#) how this access benefits you. Your story matters.





### Determination of thermoelastic stress wave propagation in nanocomposite sandwich plates reinforced by clusters of CNTs

Journal:	<i>Journal of Sandwich Structures and Materials</i>
Manuscript ID	JSSM-18-0331.R1
Manuscript Type:	Standard Article
Date Submitted by the Author:	n/a
Complete List of Authors:	Safaei, Babak; Tsinghua University, Department of Mechanical Engineering Moradi-Dastjerdi, Rasool; University of Toronto - Mississauga, Department of Mechanical and Industrial Engineering QIN, Zhaoye; Tsinghua University, Department of Mechanical Engineering Behdinan, Kamran; University of Toronto, Department of Mechanical & Industrial Engineering CHU, Fulei; Tsinghua University, Department of Mechanical Engineering
Keywords:	Stress wave propagation, Transient heat transfer, Nanocomposite sandwich plate, Carbon nanotube clusters, Impact and thermal loads, Mesh-free method
Abstract:	Adding small amounts of carbon nanotubes (CNTs) into the face sheets of sandwich structures can significantly improve their thermo-mechanical responses. However, the formation of CNT clusters, especially at high volume fractions of CNTs, dramatically affects the mechanical properties of the resulted nanocomposites, which is usually ignored. In this paper, by considering the formation of CNT clusters, we have investigated transient heat transfer and stress wave propagation in polymeric sandwich plates with two nanocomposite face sheets. The face sheets were made of clusters of CNTs embedded in a polymeric matrix. The volume fractions of CNTs and their clusters were assumed to be functionally graded (FG) along the thickness of face sheets. The proposed sandwich plate was subjected to thermal and impact pressure loads. Eshelby-Mori-Tanaka's approach was applied to evaluate the

1  
2  
3  
4  
5  
6  
7  
8  
9  
10  
11  
12  
13  
14  
15  
16  
17  
18  
19  
20  
21  
22  
23  
24  
25  
26  
27  
28  
29  
30  
31  
32  
33  
34  
35  
36  
37  
38  
39  
40  
41  
42  
43  
44  
45  
46  
47  
48  
49  
50  
51  
52  
53  
54  
55  
56  
57  
58  
59  
60

	<p>material properties of the resulted nanocomposite with components with temperature-dependent material properties. Reddy's third order shear deformation theory (TSDT) and a moving least square (MLS) shape function-based mesh-free method were utilized for thermoelastic dynamic analysis. The effects of CNT cluster size, distribution and volume fraction as well as thermal load on the thermoelastic dynamic behavior of nanocomposite sandwich plates were investigated. It was observed that the distribution and cluster size of CNTs had significant effects on the amplitude and speed of thermoelastic stress wave propagation in the nanocomposite sandwich plates.</p>



# Determination of thermoelastic stress wave propagation in nanocomposite sandwich plates reinforced by clusters of CNTs

Babak Safaei<sup>1</sup>, Rasool Moradi-Dastjerdi<sup>2</sup>, Zhaoye Qin<sup>1</sup>, Kamran Behdinan<sup>2</sup>, Fulei Chu<sup>1\*</sup>

1. Department of Mechanical Engineering, Tsinghua University, Beijing 100084, China.

2. Advanced Research Laboratory for Multifunctional Light Weight Structures, Department of Mechanical & Industrial Engineering, University of Toronto, Toronto, Canada.

## Abstract

Adding small amounts of carbon nanotubes (CNTs) into the face sheets of sandwich structures can significantly improve their thermo-mechanical responses. However, the formation of CNT clusters, especially at high volume fractions of CNTs, dramatically affects the mechanical properties of the resulted nanocomposites, which is usually ignored. In this paper, by considering the formation of CNT clusters, we have investigated transient heat transfer and stress wave propagation in polymeric sandwich plates with two nanocomposite face sheets. The face sheets were made of clusters of CNTs embedded in a polymeric matrix. The volume fractions of CNTs and their clusters were assumed to be functionally graded (FG) along the thickness of face sheets. The proposed sandwich plate was subjected to thermal and impact pressure loads. Eshelby-Mori-Tanaka's approach was applied to evaluate the material properties of the resulted nanocomposite with components with temperature-dependent material properties. Reddy's third order shear deformation theory (TSDT) and a moving least square (MLS) shape function-based mesh-free method were utilized for thermoelastic dynamic analysis. The effects of CNT cluster size, distribution and volume fraction as well as thermal load on the thermoelastic dynamic behavior of nanocomposite sandwich plates were investigated. It was observed that the distribution and cluster size of CNTs had significant effects on the amplitude and speed of thermoelastic stress wave propagation in the nanocomposite sandwich plates.

**Keywords:** Stress wave propagation; Transient heat transfer; Nanocomposite sandwich plate; Carbon nanotube clusters; Impact and thermal loads; Mesh-free method

---

\* Corresponding author: chufli@mail.tsinghua.edu.cn, Tel: +861062792842, orcid.org/0000-0003-0775-3593

## 1. INTRODUCTION

Sandwich structures with one or two stiff face sheet(s) and a softer core usually enjoy several advantages such as high strength and stiffness along with low weight, high durability in harsh environments, fire protection (or flame retardant) and high thermal-acoustic insulation behaviors [1–3]. These advantages make them attractive for researchers and efficient candidates for different industries such as aerospace, automobile and transportation [4,5]. After Iijima discovered CNTs [6], it has been well established that CNTs have exceptional thermal and mechanical properties. Extremely high aspect ratio (usually  $>1000$ ) and Young's modulus of CNTs along with low weight make them ideal nano-filler materials to improve mechanical, electrical and thermal properties of the hosted matrix [7–9]. Therefore, the use of CNTs in face sheet(s) can remarkably improve sandwich structures and provide nanocomposite sandwich structures [10,11]. However, two important issues must be taken into account while using CNTs: (i) the formation of CNT clusters inside the matrix and (ii) cost. It has been demonstrated that the formation of CNT clusters, especially in high values of CNT volume fractions, dramatically reduces the mechanical properties of the resulted nanocomposites which is usually ignored to simplify modeling procedures [12,13]. Moreover, to reduce costs, the application of the concept of functionally graded materials (FGMs) for the distribution of CNTs would be beneficial. FGMs are a new class of composite materials in which the volume fractions of components vary continuously and uniformly through a specific profile(s) [14,15]. Considering this concept for CNT distribution can result in the optimal use of CNTs; in other words, using the minimum amount of CNTs in the resulted nanocomposite [16]. These nanocomposites are called functionally graded carbon nanotube-reinforced composites (FG-CNTRCs) and their application in sandwich structures offers wide potential engineering applications.

The estimation of the material properties of nanocomposites has been the main focus of research in this area [17–22]; While, mechanical responses of nanocomposite structures have also attracted great attentions in recent years. Zhang and Xiao [23] studied the timeline vibration response of FG-CNTRC skew plates subjected to a sudden dynamic mechanical load using first order shear deformation theory (FSDT)-based element-free IMLS-Ritz method. Kolahchi et al. [24] proposed a viscoelastic FG-CNTRC plate integrated with two piezoelectric layers and studied wave propagation in the proposed structures using a refined zigzag theory. Moradi-Dastjerdi and Momeni-Khabisi [25,26] proposed a mesh-free method based on FSDT to study stress wave propagation and forced vibration in FG-CNTRC plate and sandwich plates resting

1  
2  
3 on a two-parameter elastic foundation subjected to time-dependent mechanical loads. Bisheh  
4 and Wu [27,28] used FSDT and conducted stress wave propagation in CNT-reinforced and  
5 fiber-reinforced piezoelectric cylindrical shells considering rotary inertia. Tornabene et al. [29]  
6 investigated the static behaviors of nanocomposite shells and plates reinforced with CNTs  
7 clusters using generalized differential quadrature method (GDQM) and higher order shear  
8 deformation theory (HSDT). The free vibration behavior of rotating cylindrical shells coupled  
9 with different boundary conditions have also been performed [30,31]. Setoodeh and Shojaee  
10 [32] developed a transformed weighing coefficients DQM based on classical plate theory (CPT)  
11 to analyze nonlinear free vibration in FG-CNTRC quadrilateral plates. Ghorbanpour Arani et  
12 al. [33] applied nonlocal theory to consider size effect on the wave propagation behavior of  
13 non-classical FG-CNTRC plates integrated with two piezoelectric layers resting on a  
14 viscoelastic foundation. Furthermore, the vibration behavior of a non-uniform nanoplate [34]  
15 and 2D-FG nano-beams [35] were presented using nonlocal theory.

16  
17 In previous works, the effect of thermal loads has been usually considered with two  
18 different approaches: (i) uniform thermal load (thermal environment) and (ii) thermal gradient  
19 load. Alibeigloo [36] conducted thermo-electro-mechanical analysis on FG-CNTRC cylindrical  
20 panels integrated with two piezoelectric layers using Fourier series, state-space technique and  
21 piezo-elasticity theory. The natural frequencies of FG-CNTRC plates and sandwich plates  
22 subjected to uniform thermal environment were characterized using a finite element method  
23 based on HSDT [37,38]. Asadi [39] utilized FSDT and Donnell shell theory to investigate aero-  
24 thermoelastic flutter and buckling behavior of FG-CNTRC cylindrical shells subjected to  
25 aerodynamic loading and thermal environment. Sobhaniaragh et al. [40] considered ceramic  
26 cylindrical shells reinforced with CNTs clusters and reported their thermo-elastic responses  
27 using GDQM. Thanh et al. [41] studied the natural frequencies and deflection time histories of  
28 imperfect FG-CNTRC plates subjected to thermal environment and time-dependent mechanical  
29 loads using a method based on Airy stress function and HSDT. An axisymmetric model was  
30 developed to investigate the natural frequency and stress wave propagation responses of FG-  
31 CNTRC cylinders subjected to thermal gradient and mechanical loads [42,43]. Fazzolari [44]  
32 studied critical buckling load and natural frequencies of temperature-dependent FG-CNTRC  
33 plates using higher order theories and Ritz method. Hosseini and Zhang [45] used Green-  
34 Naghdi theory and generalized finite-difference method to present coupled thermoelastic stress  
35 wave propagation in FG multilayer graphene-reinforced nanocomposite cylinders. The  
36 transient heat transfer behaviors of FG-CNTRC cylinders [46], panels [47,48] and microbeams

[49] have also been investigated. Considering the formation of CNTs clusters, the free and forced vibration responses of nanocomposite sandwich plates with FG-CNTRC face sheets subjected to steady state thermal gradient loads were evaluated using a mesh-free method [50,51].

In this paper, the effect of CNT clusters on the mechanical properties of CNT-reinforced nanocomposites has been investigated using Eshelby-Mori-Tanaka's approach, and transient heat transfer and stress wave propagation in polymeric FG-CNTRC sandwich plates have been presented. After deriving time history of temperature distribution, temperature-dependent material properties and thermal strain were calculated. Then, thermoelastic stress wave propagation in nanocomposite sandwich plates subjected to thermal and impact pressure loads was studied. In sandwich plates, the volume fractions of CNTs and their clusters were assumed to be functionally graded along the thickness of face sheets. Reddy's TSDT was utilized to approximate the displacement field of sandwich plates and a mesh-free method based on MLS shape function was developed for thermoelastic dynamic analysis. The effects of CNTs cluster size, distribution and volume fraction as well as thermal load on the thermoelastic dynamic behavior of nanocomposite sandwich plates have been investigated.

## 2. Material Properties of Functionally Graded CNTs-Reinforced Composite

In the present work, we have considered simply supported sandwich plates consisting of a neat polymeric core and two polymeric FG nanocomposite face sheets reinforced with clusters of CNTs. Sandwich plates were assumed to be subjected to a mechanical impact load and a thermal gradient load with temperatures  $T_t$  and  $T_b$  at top and bottom surfaces, respectively, with initial sandwich plate temperature of  $T_0$ . In the proposed sandwich structures, the length and width are  $a$ , face sheet thicknesses are  $h_f$  and total thickness is  $h$ , as shown in Figure 1. FG distribution of CNTs along the thickness of face sheets ( $z$  direction) was assumed as:

$$\begin{cases} f_r = ((2z - h) / (2h_f) + 1)^n f_{(r-max)}, & z > (h / 2 - h_f) \\ f_r = 0, & (-h / 2 + h_f) < z < (h / 2 - h_f) \\ f_r = (1 - (2z + h) / (2h_f))^n f_{(r-max)}, & z < (-h / 2 + h_f) \end{cases} \quad (1)$$

where  $n$  and  $f_{(r-max)}$  are the exponent and maximum (outer surface) values of CNT volume fractions, respectively. As proposed in Equation (1), the CNT volume fractions of inner surfaces

of outer layers were set at zero to show a continuous variation of material properties from neat polymeric core to FG nanocomposite face sheets.

For randomly oriented CNTs-reinforced nanocomposites, effective thermal conductivity coefficient  $k_e$  was proposed to be [52]:

$$\frac{k_e}{k_m} = \frac{3(k_{11}^{CNT} / k_m + 1) + f_r [2((k_{11}^{CNT} / k_m) - 1) + (k_{11}^{CNT} / k_m + 1)(k_{22}^{CNT} / k_m - 1)]}{3(k_{11}^{CNT} / k_m + 1) - 2f_r (k_{11}^{CNT} / k_m - 1)} \quad (2)$$

where  $k_m$  is thermal conductivity coefficient of matrix, and  $k_{11}^{CNT}$  and  $k_{22}^{CNT}$  are its corresponding CNTs value along axial and radial directions, respectively. Moreover, the same equation was utilized to predict the effective thermal expansion coefficient  $\alpha_e$  of CNTRC.

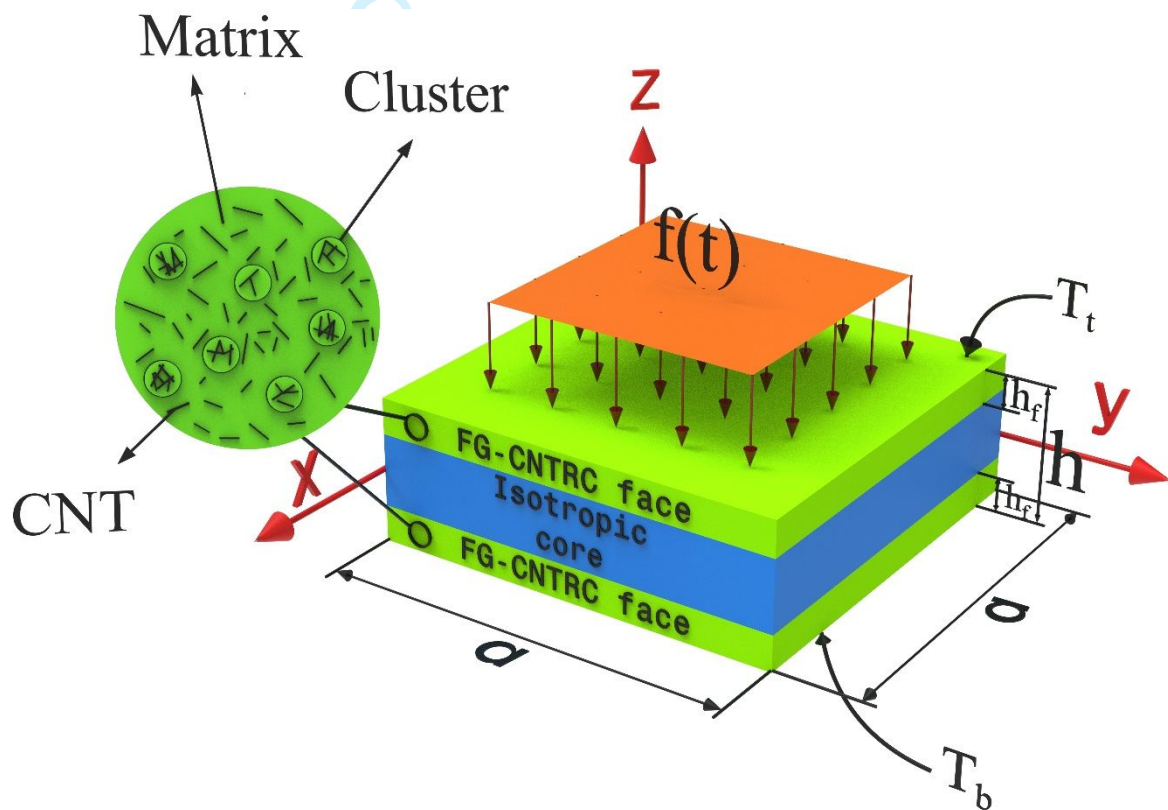


**Figure 1.** Nanocomposite sandwich plate reinforced with CNTs and their clusters

Eshelby–Mori–Tanaka’s approach was used to consider the effect of the formation of CNT clusters in nanocomposites reinforced with CNT clusters. In this approach, a representative volume element (RVE) was considered and certain amounts of randomly oriented CNTs were assumed to be located inside and outside the clusters as shown in Figure 1. For this assumption,

they defined two parameters to indicate the volume fraction of clusters inside RVE  $\mu$  and the volume fraction of CNTs inside clusters  $\eta$  as follows [53]:

$$\mu = V_{cluster} / V, \quad \eta = V_r^{cluster} / V_r \quad 0 \leq \mu, \eta \leq 1 \quad (3)$$

where  $V$ ,  $V_r$ ,  $V_{cluster}$ , and  $V_r^{cluster}$  are RVE volume, total CNTs volume of RVE, total cluster volume, and total CNTs volume inside clusters, respectively. Based on Equation (3),  $\eta=1$  denoted that all CNTs were located inside clusters and  $\mu=1$  (or  $\mu=\eta$ ) indicated fully dispersed CNTs in matrix. For inside and outside clusters, Eshelby–Mori–Tanaka's approach proposed the effective definitions of bulk modulus  $K$  and shear modulus  $G$  as follows [53–55]:

$$K_{in} = K_m + \frac{f_r \eta (\delta_r - 3K_m \alpha_r)}{3(\mu - f_r \eta + f_r \eta \alpha_r)}, \quad G_{in} = G_m + \frac{f_r \eta (\eta_r - 3G_m \beta_r)}{2(\eta_r - 3G_m \beta_r)} \quad (4)$$

$$K_{out} = K_m + \frac{f_r (1-\eta) (\delta_r - 3K_m \alpha_r)}{3[1-\mu - f_r (1-\eta) + f_r (1-\eta) \alpha_r]}, \quad G_{out} = G_m + \frac{f_r (1-\eta) (\eta_r - 2G_m \beta_r)}{2[1-\mu - f_r (1-\eta) + f_r (1-\eta) \beta_r]} \quad (5)$$

where subscript  $m$  is applied for matrix material and:

$$\alpha_r = \frac{3(K_m + G_m) + k_r - l_r}{3(K_m + k_r)} \quad (6)$$

$$\beta_r = \frac{1}{5} \left\{ \frac{4G_m + 2k_r + l_r}{3(G_m + k_r)} + \frac{4G_m}{G_m + p_r} + \frac{2[G_m(3K_m + G_m) + G_m(3K_m + 7G_m)]}{G_m(3K_m + G_m) + m_r(3K_m + 7G_m)} \right\} \quad (7)$$

$$\delta_r = \frac{1}{3} \left\{ n_r + 2l_r + \frac{(2k_r + l_r) + (3K_m + 2G_m - l_r)}{G_m + k_r} \right\} \quad (8)$$

$$\eta_r = \frac{1}{5} \left[ \frac{2}{3} (n_r - l_r) + \frac{8G_m p_r}{G_m + p_r} + \frac{8m_r G_m (3K_m + 4G_m)}{3K_m (m_r + G_m) + G_m (7m_r + G_m)} + \frac{2(k_r - l_r)(2G_m + l_r)}{3(G_m + k_r)} \right] \quad (9)$$

where  $k_r$ ,  $l_r$ ,  $m_r$ ,  $n_r$ , and  $p_r$  are Hill's elastic moduli of reinforcing phase (CNTs) defined in references [53–55]. Finally, Mori-Tanaka's method estimates the effective mechanical properties of nanocomposite as:

$$K = K_{out} \left[ 1 + \frac{\mu \left( \frac{K_{in}}{K_{out}} - 1 \right)}{1 + \alpha(1-\mu) \left( \frac{K_{in}}{K_{out}} - 1 \right)} \right], \quad G = G_{out} \left[ 1 + \frac{\mu \left( \frac{G_{in}}{G_{out}} - 1 \right)}{1 + \beta(1-\mu) \left( \frac{G_{in}}{G_{out}} - 1 \right)} \right] \quad (10)$$

with

$$\nu_{out} = \frac{3K_{out} - 2G_{out}}{2(3K_{out} + G_{out})}, \alpha = \frac{1 + \nu_{out}}{3(1 - \nu_{out})}, \beta = \frac{2(4 - 5\nu_{out})}{15(1 - \nu_{out})} \quad (11)$$

### 3. Governing Equations

Assuming thermally isolated side faces and uniform temperatures for outer surfaces of sandwich plates gives one-dimensional heat conduction for the governing transient heat transfer equation. Transient heat transfer equation for FG nanocomposite sandwich plates can be written as [49]:

$$\frac{\partial}{\partial z} \left( k_e(z) \frac{\partial T(z,t)}{\partial z} \right) = \rho(z) c_p(z) \frac{\partial T(z,t)}{\partial t} \quad (12)$$

where  $T(z,t)$  is temperature at time  $t$  and location (along thickness)  $z$ ,  $c_p$  is specific heat conduction and  $\rho$  is density for the proposed sandwich plates. Solving this equation gave the time histories of temperature distribution in nanocomposite sandwich plates. Using time and location-dependent temperature, mechanical dynamic equation could be solved.

The governing dynamic equation of sandwich plates subjected to time-dependent mechanical loads  $f(t)$  can be derived from total energy function  $U$  as:

$$U = \frac{1}{2} \int_V \left[ \boldsymbol{\varepsilon}^T \boldsymbol{\sigma} + \boldsymbol{\gamma}^T \boldsymbol{\tau} - \rho(z)(u\boldsymbol{\varepsilon}^2 + v\boldsymbol{\varepsilon}^2 + w\boldsymbol{\varepsilon}^2) \right] dV + \int_A [f(t)w] dA \quad (13)$$

where  $A$  is a part of solution domain  $V$  with external mechanical forces and based on plate theories,  $\boldsymbol{\sigma}$ ,  $\boldsymbol{\tau}$ ,  $\boldsymbol{\varepsilon}$  and  $\boldsymbol{\gamma}$  are the vectors of reduced in-plane stress, out of plane stress, in-plane strain and out of plane strain, respectively. Also,  $u$ ,  $v$  and  $w$  are the components of estimated displacement field along  $x$ ,  $y$  and  $z$  directions, respectively.

In this work, Reddy's third order shear deformation plate theory [56] was utilized to estimate the components of displacement as follows:

$$\begin{aligned}
 u(x, y, z) &= u_0(x, y) + z \theta_x(x, y) + z^3 c_1 (\theta_x + w_{0,x}) \\
 v(x, y, z) &= v_0(x, y) + z \theta_y(x, y) + z^3 c_1 (\theta_y + w_{0,y}) \\
 w(x, y, z) &= w_0(x, y)
 \end{aligned} \tag{14}$$

where  $c_1 = -4/3h^2$ ,  $u_0$ ,  $v_0$  and  $w_0$  are mid-plane displacements.  $\theta_x$  and  $\theta_y$  represent rotations normal to mid-plane around  $y$ - and  $x$ -axes, respectively. Using Reddy's TSDT, the relation between total structural strain  $\mathbf{e} = \{\mathbf{e}_b \quad \boldsymbol{\gamma}\}^T$  and displacement components were derived as follows:

$$\mathbf{e}_b = \{e_{xx} \quad e_{yy} \quad \gamma_{xy}\}^T = \mathbf{e}_0 + z \mathbf{k}_1 + c_1 z^3 \mathbf{k}_3, \quad \boldsymbol{\gamma} = \{\gamma_{xz} \quad \gamma_{yz}\}^T = (1 + 3c_1 z^2) \boldsymbol{\gamma}_0 \tag{15}$$

where

$$\mathbf{e}_0 = \begin{Bmatrix} u_{0,x} \\ v_{0,y} \\ u_{0,y} + v_{0,x} \end{Bmatrix}, \quad \mathbf{k}_1 = \begin{Bmatrix} \theta_{x,x} \\ \theta_{y,y} \\ \theta_{x,y} + \theta_{y,x} \end{Bmatrix}, \quad \mathbf{k}_3 = \begin{Bmatrix} \theta_{x,x} + w_{0,xx} \\ \theta_{y,y} + w_{0,yy} \\ \theta_{x,y} + \theta_{y,x} + 2w_{0,xy} \end{Bmatrix}, \quad \boldsymbol{\gamma}_0 = \begin{Bmatrix} \theta_x + w_{0,x} \\ \theta_y + w_{0,y} \end{Bmatrix} \tag{16}$$

For thermoelastic problems, the in-plane part of total structural strain  $\mathbf{e}_b$  consisted of elastic strain  $\boldsymbol{\varepsilon}$  and thermal strain  $\boldsymbol{\varepsilon}_T$  which are related by  $\mathbf{e}_b = \boldsymbol{\varepsilon} + \boldsymbol{\varepsilon}_T$  and are defined as:

$$\boldsymbol{\varepsilon} = [\varepsilon_x, \varepsilon_y, \gamma_{xy}]^T, \quad \boldsymbol{\varepsilon}_T = [\alpha_e \Delta T, \alpha_e \Delta T, 0]^T \tag{17}$$

where  $\Delta T$  is the difference of sandwich plate temperature and thermal strain free temperature (300 K).

Moreover, the relationship between reduced stress and strain vectors for temperature and location-dependent nanocomposite sandwich plates are given as:

$$\begin{aligned}
 \begin{Bmatrix} \sigma_x \\ \sigma_y \\ \sigma_{xy} \end{Bmatrix} &= \begin{bmatrix} Q_{11}(z, T) & Q_{12}(z, T) & 0 \\ Q_{12}(z, T) & Q_{22}(z, T) & 0 \\ 0 & 0 & Q_{66}(z, T) \end{bmatrix} \begin{Bmatrix} \varepsilon_x \\ \varepsilon_y \\ \gamma_{xy} \end{Bmatrix} \text{ or } \boldsymbol{\sigma} = \mathbf{Q}_b(z, T) \boldsymbol{\varepsilon} \\
 \begin{Bmatrix} \sigma_{xz} \\ \sigma_{yz} \end{Bmatrix} &= \begin{bmatrix} Q_{55}(z, T) & 0 \\ 0 & Q_{44}(z, T) \end{bmatrix} \begin{Bmatrix} \gamma_{xz} \\ \gamma_{yz} \end{Bmatrix} \text{ or } \boldsymbol{\tau} = \mathbf{Q}_s(z, T) \boldsymbol{\gamma}
 \end{aligned} \tag{18}$$

where  $Q_{ij}(z, T)$  are the components of stiffness matrix in the governing constitutive equation.

#### 4. Mesh-Free Numerical Analysis

The utilized mesh-free method is based on MLS shape functions. Using these shape functions, displacement field  $\mathbf{d}$  in total energy function and the equation of motion can be approximated as follows [57]:

$$\hat{\mathbf{d}} = \left[ \hat{u}_{0i}, \hat{v}_{0i}, \hat{w}_{0i}, \hat{\theta}_{xi}, \hat{\theta}_{yi} \right]^T = \sum_{i=1}^N \phi_i d_i \quad (19)$$

where  $N$ ,  $\hat{\mathbf{d}}$  and  $\phi_i$  are the total number of nodes, virtual nodal values of displacement vector and MLS shape function for a node located at  $\mathbf{X}(x,y)=\mathbf{X}_i$ , respectively. The definition of MLS shape function is given as:

$$\phi_i(\mathbf{X}) = \mathbf{P}^T(\mathbf{X}) \mathbf{H}(\mathbf{X})^{-1} W_i(\mathbf{X} - \mathbf{X}_i) \mathbf{P}(\mathbf{X}_i) \quad (20)$$

where  $W$ ,  $\mathbf{P}$  and  $\mathbf{H}$  are cubic spline weight function, base vector, and moment matrix, respectively, which can be defined as:

$$\mathbf{P}(\mathbf{X}) = [1, x, y, xy, x^2, y^2]^T, \quad \mathbf{H}(\mathbf{X}) = \left[ \sum_{i=1}^n W(\mathbf{X} - \mathbf{X}_i) \mathbf{P}(\mathbf{X}_i) \mathbf{P}^T(\mathbf{X}_i) \right] \quad (21)$$

Utilization of MLS Shape function and TSDT, displacement field (Eq. 14) and strain vectors (Eq. 15) can be rewritten as:

$$\hat{\mathbf{u}} = \{ \hat{u}_i \quad \hat{v}_i \quad \hat{w}_i \}^T = \{ \mathbf{N}_0 + z \mathbf{N}_1 + c_1 z^3 \mathbf{N}_3 \} \hat{\mathbf{d}} \quad (22)$$

$$\mathbf{e}_b = \{ \mathbf{B}_0 + z \mathbf{B}_1 + c_1 z^3 \mathbf{B}_3 \} \hat{\mathbf{d}}, \quad \boldsymbol{\gamma} = (1 + 3c_1 z^2) \mathbf{B}_s \hat{\mathbf{d}} \quad (23)$$

where:

$$\mathbf{N}_0 = \begin{bmatrix} \varphi_i & 0 & 0 & 0 & 0 \\ 0 & \varphi_i & 0 & 0 & 0 \\ 0 & 0 & \varphi_i & 0 & 0 \end{bmatrix}, \quad \mathbf{N}_1 = \begin{bmatrix} 0 & 0 & 0 & \varphi_i & 0 \\ 0 & 0 & 0 & 0 & \varphi_i \\ 0 & 0 & 0 & 0 & 0 \end{bmatrix}, \quad \mathbf{N}_3 = \begin{bmatrix} 0 & 0 & \varphi_{i,x} & \varphi_i & 0 \\ 0 & 0 & \varphi_{i,y} & 0 & \varphi_i \\ 0 & 0 & 0 & 0 & 0 \end{bmatrix} \quad (24)$$

$$\mathbf{B}_0 = \begin{bmatrix} \varphi_{i,x} & 0 & 0 & 0 & 0 \\ 0 & \varphi_{i,y} & 0 & 0 & 0 \\ \varphi_{i,y} & \varphi_{i,x} & 0 & 0 & 0 \end{bmatrix}, \quad \mathbf{B}_1 = \begin{bmatrix} 0 & 0 & 0 & \varphi_{i,x} & 0 \\ 0 & 0 & 0 & 0 & \varphi_{i,y} \\ 0 & 0 & 0 & \varphi_{i,y} & \varphi_{i,x} \end{bmatrix}, \quad (25)$$

$$\mathbf{B}_3 = \begin{bmatrix} 0 & 0 & \varphi_{i,xx} & \varphi_{i,x} & 0 \\ 0 & 0 & \varphi_{i,yy} & 0 & \varphi_{i,y} \\ 0 & 0 & 2\varphi_{i,xy} & \varphi_{i,y} & \varphi_{i,x} \end{bmatrix}, \quad \mathbf{B}_s = \begin{bmatrix} 0 & 0 & \varphi_{i,x} & \varphi_i & 0 \\ 0 & 0 & \varphi_{i,y} & 0 & \varphi_i \end{bmatrix}$$

Moreover,  $\boldsymbol{\varphi}_w$  is defined for the application of mechanical load along thickness as:

$$\boldsymbol{\varphi}_w = [0 \quad 0 \quad \varphi_i \quad 0 \quad 0] \quad (26)$$

Using the relation of total structural strain ( $\mathbf{e} = \boldsymbol{\varepsilon} + \boldsymbol{\varepsilon}_T$ ) and the substitution of equations (19) and (22) - (26) into total energy equation (Eq. 13), give:

$$\begin{aligned} U = & -\frac{1}{2} \int_A \hat{\mathbf{d}}^T \begin{bmatrix} \mathbf{N}_0^T & \mathbf{N}_1^T & \mathbf{N}_3^T \end{bmatrix} \overline{\mathbf{M}} \begin{bmatrix} \mathbf{N}_0 & \mathbf{N}_1 & \mathbf{N}_3 \end{bmatrix}^T \hat{\mathbf{d}} dA \\ & + \frac{1}{2} \int_A \hat{\mathbf{d}}^T \begin{bmatrix} \mathbf{B}_0^T & \mathbf{B}_1^T & \mathbf{B}_3^T \end{bmatrix} \overline{\mathbf{Q}}_b \begin{bmatrix} \mathbf{B}_0 & \mathbf{B}_1 & \mathbf{B}_3 \end{bmatrix}^T \hat{\mathbf{d}} dA \\ & + \frac{1}{2} \int_A \hat{\mathbf{d}}^T \begin{bmatrix} \mathbf{B}_s^T & \mathbf{B}_s^T \end{bmatrix} \overline{\mathbf{Q}}_s \begin{bmatrix} \mathbf{B}_s & \mathbf{B}_s \end{bmatrix}^T \hat{\mathbf{d}} dA - \int_A \hat{\mathbf{d}}^T \begin{bmatrix} \mathbf{B}_0^T & \mathbf{B}_1^T & \mathbf{B}_3^T \end{bmatrix} \overline{\mathbf{Q}}_a dA + \int_A \boldsymbol{\varphi}_w^T f(t) dA \end{aligned} \quad (27)$$

where

$$\begin{aligned} \overline{\mathbf{Q}}_b = \int_{-h/2}^{h/2} \begin{bmatrix} 1 & z & c_1 z^3 \\ & z^2 & c_1 z^4 \\ Sym. & & c_1^2 z^6 \end{bmatrix} \mathbf{Q}_b dz, \quad \overline{\mathbf{Q}}_s = \int_{-h/2}^{h/2} \begin{bmatrix} 1 & 3c_1 z^2 \\ 3c_1 z^2 & 9c_1^2 z^4 \end{bmatrix} \mathbf{Q}_s dz, \\ \overline{\mathbf{M}} = \int_{-h/2}^{h/2} \begin{bmatrix} 1 & z & c_1 z^3 \\ & z^2 & c_1 z^4 \\ Sym. & & c_1^2 z^6 \end{bmatrix} \rho(z) dz, \quad \overline{\mathbf{Q}}_a = \int_{-h/2}^{h/2} \begin{Bmatrix} 1 \\ z \\ c_1 z^3 \end{Bmatrix} \mathbf{Q}_b \boldsymbol{\varepsilon}_T dz \end{aligned} \quad (28)$$

Finally, by derivation with respect to displacement vector  $\hat{\mathbf{d}}$  (applying Hamilton's principle), Equation (27) can be rewritten as:

$$\mathbf{M}\dot{\hat{\mathbf{d}}} + \mathbf{K}\hat{\mathbf{d}} = \mathbf{f}_m + \mathbf{f}_T \quad (29)$$

where,  $\mathbf{M}$ ,  $\mathbf{K}$ ,  $\mathbf{f}_m$ , and  $\mathbf{f}_T$  are mass matrix, stiffness matrix, mechanical force vector and resultant thermal force vector, respectively, which are defined as:

$$\mathbf{M} = \int_A \begin{bmatrix} \mathbf{N}_0^T & \mathbf{N}_1^T & \mathbf{N}_3^T \end{bmatrix} \overline{\mathbf{M}} \begin{bmatrix} \mathbf{N}_0 & \mathbf{N}_1 & \mathbf{N}_3 \end{bmatrix}^T dA \quad (30)$$

$$\mathbf{K} = \int_A \begin{bmatrix} \mathbf{B}_0^T & \mathbf{B}_1^T & \mathbf{B}_3^T \end{bmatrix} \overline{\mathbf{Q}}_b \begin{bmatrix} \mathbf{B}_0 & \mathbf{B}_1 & \mathbf{B}_3 \end{bmatrix}^T dA + \int_A \begin{bmatrix} \mathbf{B}_s^T & \mathbf{B}_s^T \end{bmatrix} \overline{\mathbf{Q}}_s \begin{bmatrix} \mathbf{B}_s & \mathbf{B}_s \end{bmatrix}^T dA \quad (31)$$

$$\mathbf{f}_m = \int_A \boldsymbol{\varphi}_w^T f(t) dA, \quad \mathbf{f}_T = - \int_A \begin{bmatrix} \mathbf{B}_0^T & \mathbf{B}_1^T & \mathbf{B}_3^T \end{bmatrix} \overline{\mathbf{Q}}_a dA \quad (32)$$

The time dependent system of discretized Equation (29) were solved using Newmark (central difference) method.

Utilization of the same trend, the mesh-free discretized equation of transient heat transfer in nanocomposite sandwich plates can be presented as:

$$\mathbf{C} \frac{\partial \hat{\mathbf{T}}}{\partial t} + \mathbf{k}_T \hat{\mathbf{T}} = \mathbf{q} \quad (33)$$

where

$$\mathbf{C} = \int_A (\rho c_p) \Phi_T^T \Phi_T dV, \mathbf{k}_T = \int_V \mathbf{B}_T^T k_e(z) \mathbf{B}_T dV, \mathbf{q} = \int_A \Phi_T^T \mathbf{Q}_T dA, \hat{\mathbf{T}} = [\hat{T}_1 \quad \hat{T}_2 \quad \dots \quad \hat{T}_N]^T \quad (34)$$

with

$$\Phi_T = [\Phi_1 \quad \Phi_2 \quad \dots \quad \Phi_N]^T, \mathbf{B}_T = \left[ \frac{\partial \Phi_1}{\partial z} \quad \frac{\partial \Phi_2}{\partial z} \quad \dots \quad \frac{\partial \Phi_N}{\partial z} \right]^T \quad (35)$$

It should be noted that, since MLS shape functions did not satisfy Kronecker delta property, essential boundary conditions were imposed by transformation method which regenerated Equations. (29) and (33) based on real nodal values of displacement  $\mathbf{d}$  and temperature  $\mathbf{T}$  instead of virtual ones ( $\hat{\mathbf{d}}$  and  $\hat{\mathbf{T}}$ ) [26].

## 5. Results and discussions

The validation of the developed methods, transient heat transfer and thermoelastic stress wave propagations for the proposed FG nanocomposite sandwich plates have been presented in this section. The polymeric isotropic core of the proposed sandwich plates was made of PMMA and nanocomposite face sheets were assumed to be reinforced with armchair (10, 10) single-walled CNTs ( $L=9.26$  nm,  $R=0.68$  nm,  $h=0.067$  nm). Temperature-dependent material properties of CNTs are reported in Table 1 [16] and for other temperatures, they were estimated by the best fit third-degree polynomials as:

$$P = P_1 T^3 + P_2 T^2 + P_3 T + P_4 \quad (36)$$

where  $P$  can be used for each property reported in Table 1 and  $P_i$  ( $i=1,2,3,4$ ) is constant values of predicted polynomials. Moreover, the temperature-dependent material properties of PMMA were estimated as:

$$E_m = (3.52 - 0.0034T) \text{ GPa}, \alpha_m = 45(1 + 0.0005\Delta T) \times 10^{-6} / K \quad (37)$$

where at strain free temperature ( $T_0 = 300 K$ ), we have  $E_m = 2.5 \text{ GPa}$  and  $\alpha_m = 45 \times 10^{-6} / K$ . Other material properties of PMMA and SWCNTs were considered **to be** as follows [16,43]:

PMMA:  $\nu_m = 0.34$ ,  $\rho_m = 1150 \text{ Kg/m}^3$ ,  $k_m = 0.247 \text{ W/mK}$  and  $c_p^{CNT} = 1466 \text{ J/Kg.K}$

SWCNT:  $\nu_{12}^{CNT} = 0.175$ ,  $\rho^{CNT} = 1400 \text{ Kg/m}^3$ ,  $k_{11}^{CN} = 3000 \text{ W/mK}$ ,  $k_{22}^{CN} = 100 \text{ W/mK}$  and  $c_p^{CNT} = 600 \text{ j/Kg.K}$

**Table 1.** Temperature-dependent material properties of armchair (10,10) SWCNT [16]

$T$ (K)	$E_{11}^{CN}$ (GPa)	$E_{22}^{CN}$ (GPa)	$G_{12}^{CN}$ (GPa)	$\alpha_{11}^{CN}$ ( $10^{-6}/K$ )	$\alpha_{22}^{CN}$ ( $10^{-6}/K$ )
300	5646.6	7080	1944.5	3.4584	5.1682
400	5667.9	6981.4	1970.3	4.1496	5.0905
500	5530.8	6934.8	1964.3	4.5361	5.0189
700	5474.4	6864.1	1964.4	4.6677	4.8943

### 5.1. Validation of models

In this section, the accuracy of the developed mesh-free method for both heat transfer and dynamic problems were examined.

For heat transfer problems, we assumed a square FG-CNTRC plate and a sandwich plate with  $h/a=0.01$ ,  $h_f/h=0.2$ ,  $f_{r-max}=0.2$ ,  $n=10$ ,  $T_i=450 \text{ K}$  and  $T_b=350 \text{ K}$  at initial temperature  $T_0=300 \text{ K}$ . Figure 2 shows that temperature distributions along the thickness of the considered plate and sandwich plate were gradually converged to those obtained from steady state heat transfer problems. Excellent agreements were observed between the results obtained for steady state problems and the stationary results of transient heat transfer problems for both square plate and sandwich plate.

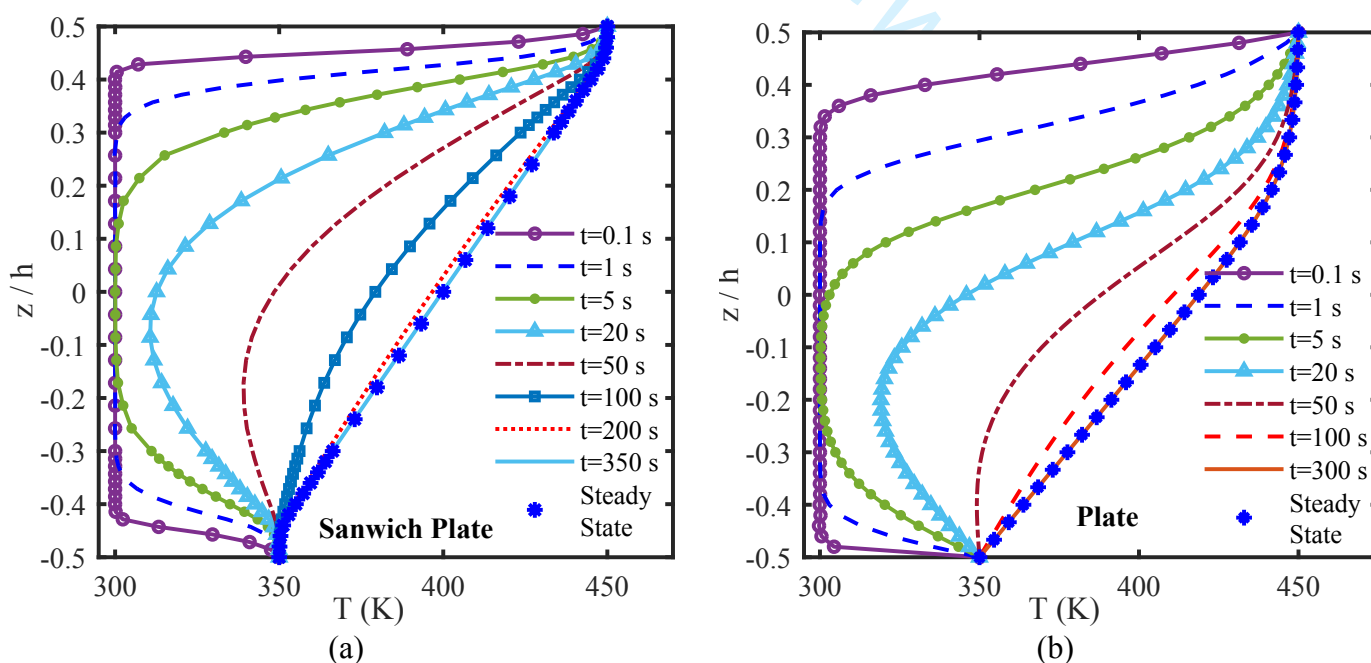


**Figure 2.** Comparison of predicted temperature distributions along the thickness of square FG-CNTRC (a) plate and (b) sandwich plate with  $h/a=0.01$ ,  $h_f/h=0.2$ ,  $f_{r-max}=0.2$ ,  $n=10$ ,  $T_i=450$  K,  $T_b=350$  K and  $T_0=300$  K at different times with steady state results

In order to examine the convergence and accuracy of the developed mesh-free method in terms of dynamic results, the vibration of an isotropic square simply supported plate subjected to an impact pressure load was compared with those reported in [58]. They used Navier solution and first order shear deformation theory to derive time histories of vibration for the plate with  $E=3$  GPa,  $\nu=0.34$ ,  $\rho=1200$  Kg / m<sup>3</sup>,  $h/a=0.1$ ,  $a=0.45$  m and impact load as [58]:

$$f(t) = \begin{cases} P_{\max} (1 - t/t_p) & 0 \leq t \leq t_p \\ 0 & t < 0 \text{ and } t > t_p \end{cases} \quad (38)$$

where  $P_{\max} = 200$  kPa and  $t = 10$  ms. Figure 3 compares the results reported in [58] with those of developed method with  $5 \times 5$ ,  $7 \times 7$ ,  $9 \times 9$  and  $17 \times 17$  node distributions. A very good accuracy was provided by  $17 \times 17$  node arrangement. Furthermore, the increase of node numbers from 9 to 17 had an insignificant effect on the accuracy of results which showed the convergence of results.

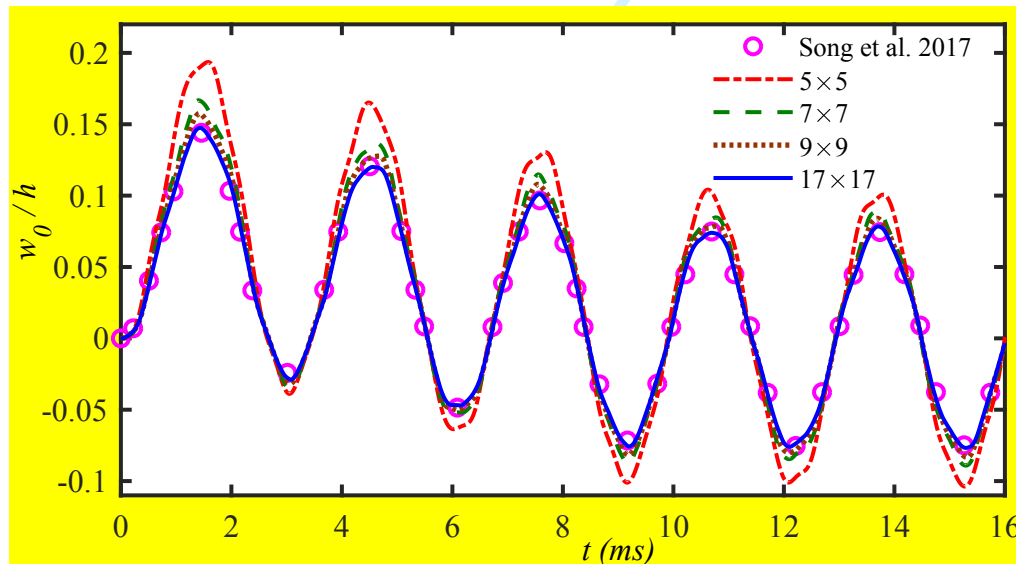


**Figure 3.** Comparison between the results reported in [58] and those obtained from the developed mesh-free method for central point vibration of isotropic plate

It is worth noting that in the following dynamic analyses of sandwich plates,  $15 \times 15$  node arrangement and  $14 \times 14$  background cells were adopted for the integration of local mass and stiffness matrices with 4 Gauss points in each cell.

## 5.2. Transient heat transfer in FG-CNTRC sandwich plates

In this section, we have investigated the effects of volume fraction and distribution of CNTs on the time-dependent heat transfer of the proposed square nanocomposite plates and sandwich plates with  $h/a=0.01$ ,  $T_t=450$  K,  $T_b=350$  K and  $T_0=300$  K. Figures 4 and 5 illustrate stationary temperature distributions and time histories of temperature at mid node of sandwich plates with  $h_f/h=0.2$  for  $f_{r-max}=0.1$  and  $f_{r-max}=0.2$ , respectively. It was observed that the decrease of CNT volume fractions exponent  $n$  or increase of  $f_{r-max}$ , due to the increase of the total volume of consumed CNTs, improved thermal conductivity of the sandwich plates. It meant that temperatures at nanocomposite face sheets with lower  $n$  or higher  $f_{r-max}$  values were closer to their outer surface temperatures. Moreover, increasing CNT volume fractions reduced the time required for the stationary condition to be achieved.

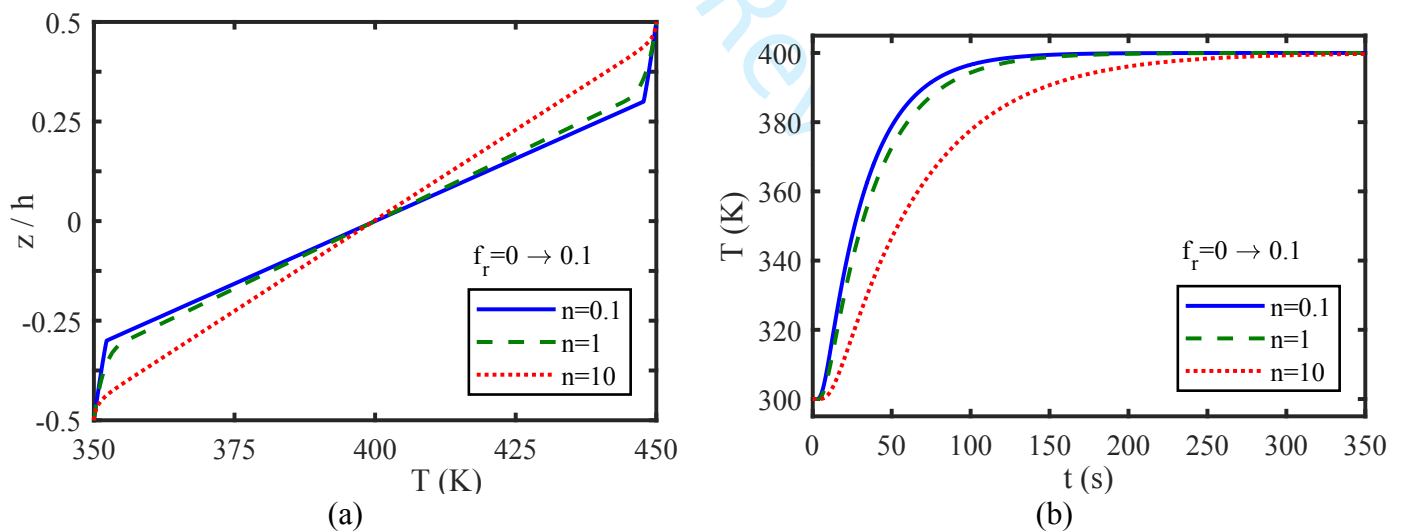


**Figure 4.** (a) stationary temperature distributions (b) time histories of temperature at mid node of sandwich plates with  $h/a=0.01$ ,  $h_f/h=0.2$ ,  $T_t=450$  K,  $T_b=350$  K,  $T_0=300$  K and  $f_{r-max}=0.1$

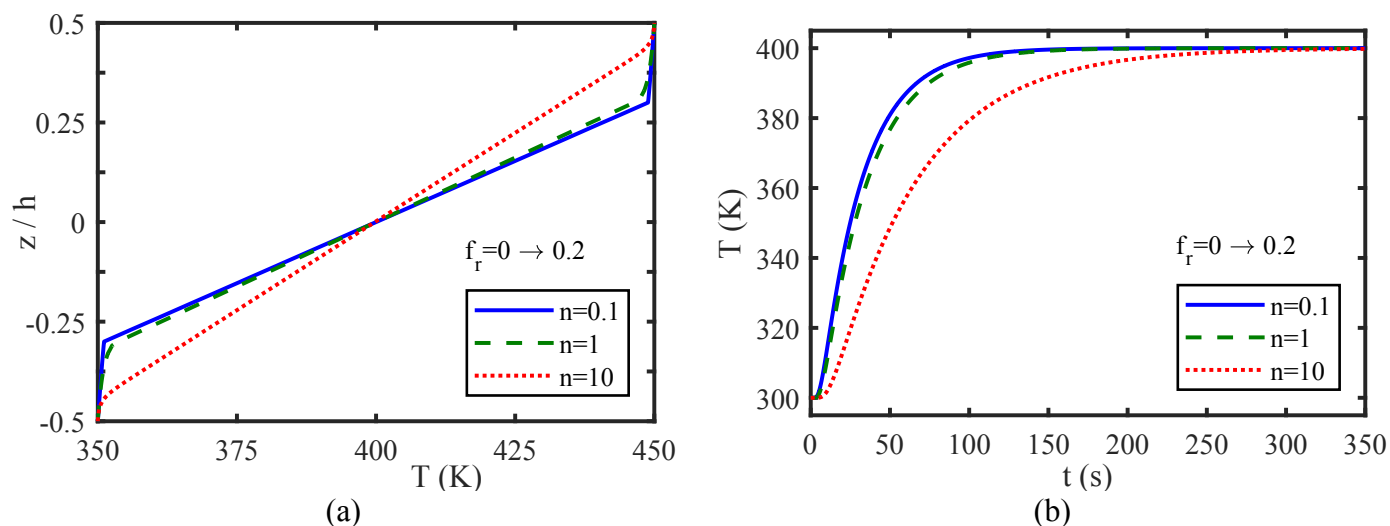


**Figure 5.** (a) stationary temperature distributions (b) time histories of temperature at mid node of sandwich plates with  $h/a=0.01$ ,  $h_f/h=0.2$ ,  $T_t=450$  K,  $T_b=350$  K,  $T_0=300$  K and  $f_{r-max}=0.2$

In addition, Figure 6 shows the same results for nanocomposite plates with  $f_{r-max}=0.2$ . This figure shows that CNT distribution had a significant effect on the temperature distribution and stationary time of FG-CNTRC plates such that decreasing  $n$  led to a more linear temperature distribution and the reduction of stationary time of nanocomposite plates. Moreover, comparing Figure 6 with Figure 5 showed that the stationary time of sandwich plates were much longer than plates with the same thicknesses.

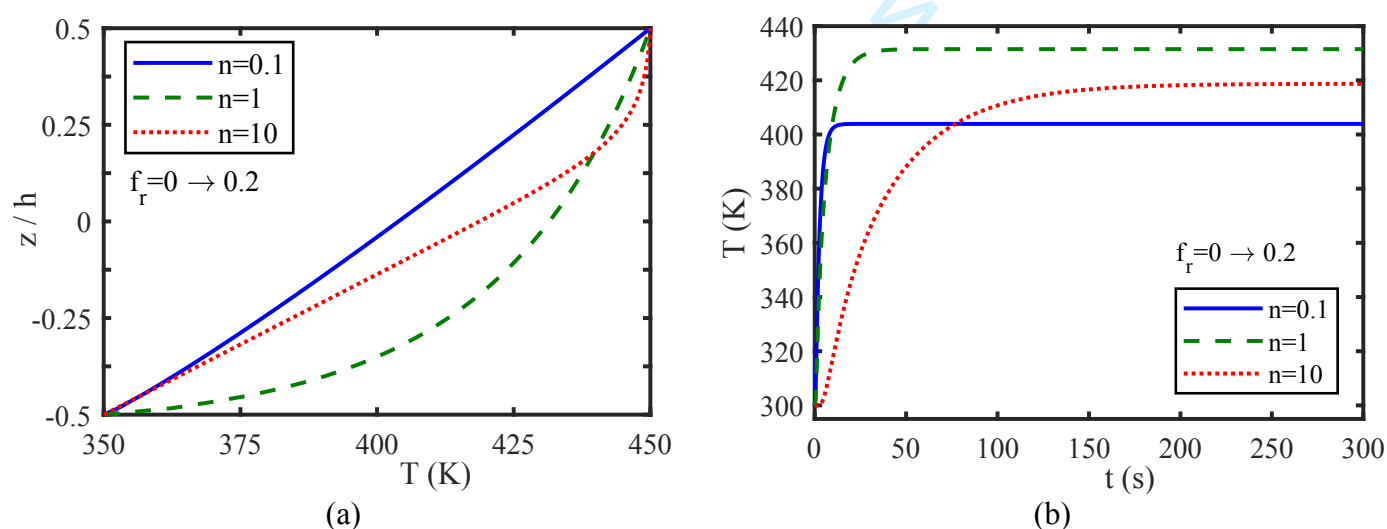
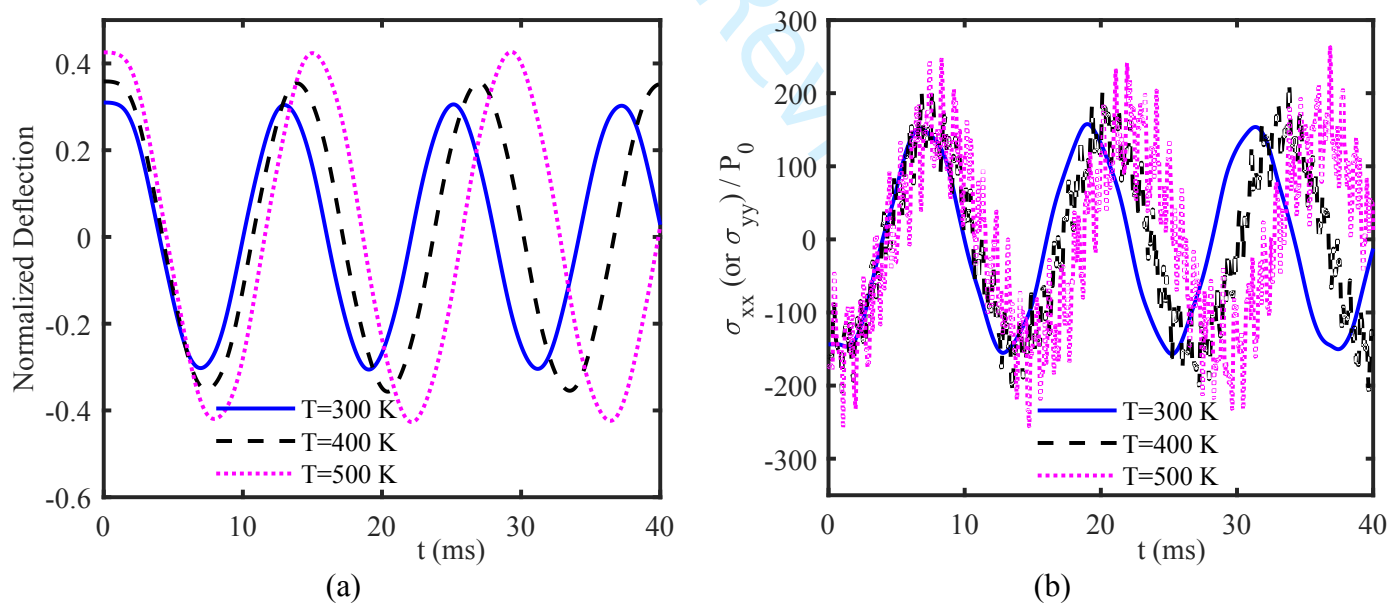


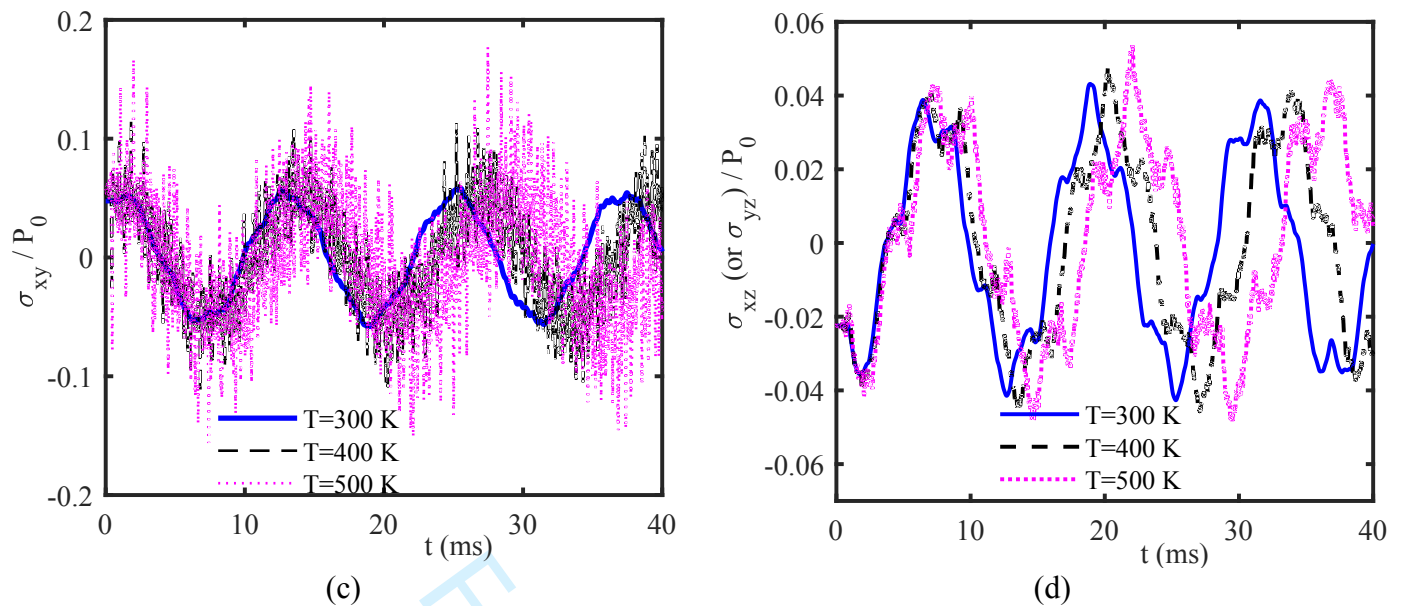
**Figure 6.** (a) stationary temperature distributions (b) time histories of temperature at mid node of plates with  $h/a=0.01$ ,  $T_t=450$  K,  $T_b=350$  K,  $T_0=300$  K and  $f_{r-max}=0.2$

### 5.3. Stress wave propagation in FG-CNTRC sandwich plates

In this section, we have investigated the thermoelastic vibration and stress wave propagations of simply supported square nanocomposite sandwich plates with  $h/a=0.05$  and  $h_f/h=0.1$  subjected to a thermal environment and the same pressure impact load (Eq. 38) with  $t_m=2$  ms and  $P_0=1$  MPa. It should be mentioned that  $\hat{q} = 10E_m h^3 q / f_0 a^4$  was considered as the normalized value of deflections in the following simulations.

The effect of environment temperature on the thermoelastic dynamic behavior of the central node of the nanocomposite sandwich plates reinforced with uniformly distributed (UD) CNTs with  $\mu=0.3$ ,  $\eta=1$  and  $f_r=0.2$  is shown in Figure 7. These figures showed that, due to decreasing the stiffness of sandwich plates, the rising temperature led to increase in the amplitudes and reduction in the speeds of wave propagations. Moreover, thermal environment caused lots of fluctuations in stress wave propagations. Furthermore, comparing the amplitudes of normal and shear stresses revealed that the values of normal stresses were much higher than the values of shear stresses, especially those were out of plane.

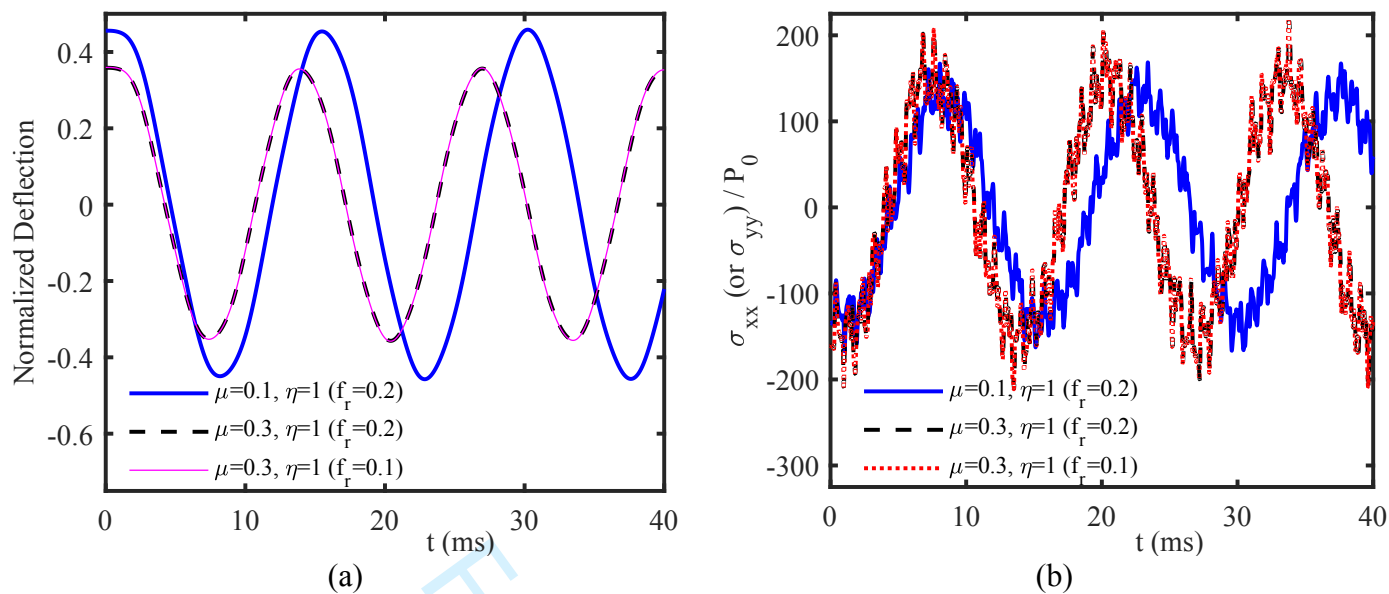




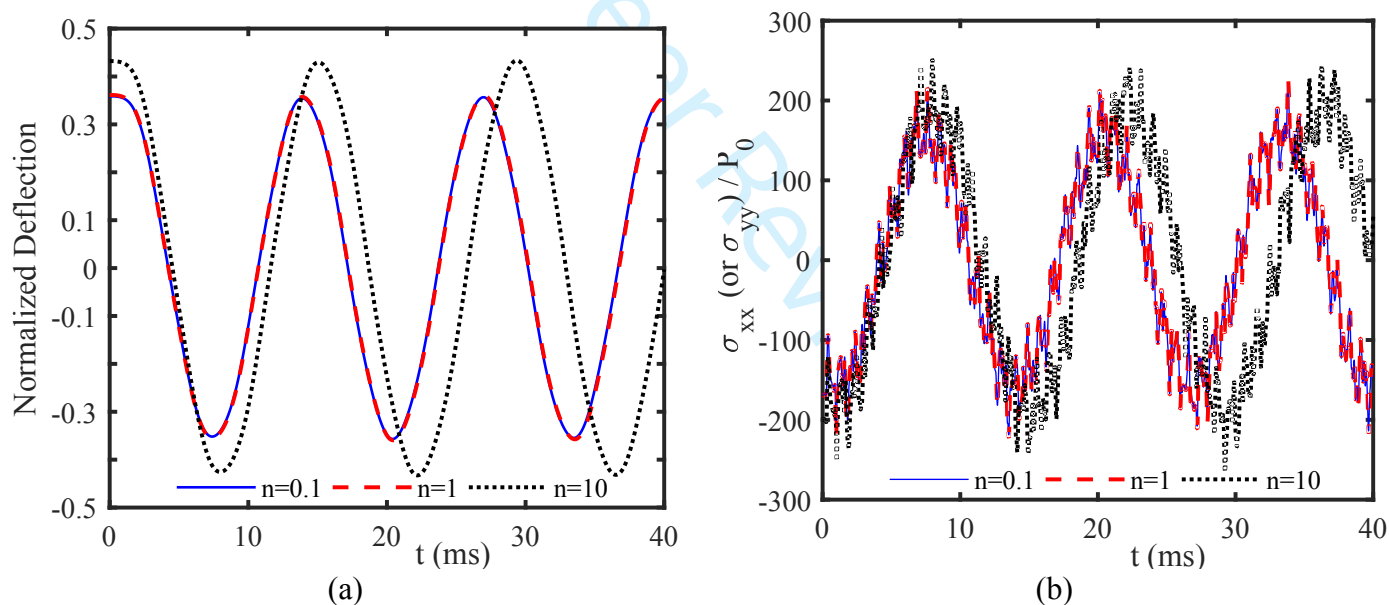
**Figure 7.** Time histories of thermoelastic (a) deflection (b) normal stresses (c) in plane shear stress and (d) out of plane shear stresses in nanocomposite sandwich plates with  $h/a=0.05$ ,  $h_f/h=0.1$ ,  $\mu=0.3$ ,  $\eta=1$  and  $f_r=0.2$

Figure 8 explores the effect of cluster sizes,  $\mu$ , and CNT volume fraction on the time histories of deflection and normal stress of the prepared sandwich plates at environment temperature of  $T=400$  K. Although CNT volume fraction did not have a significant effect, it was observed that expanding of the size of CNT clusters led to a considerable reduction in the amplitude and remarkable increase in the speed of wave propagations. These observations were due to the effects of these two parameters on the material properties of the resulted nanocomposite.

The effect of CNT distribution on the stress wave propagation of the same FG-CNTRC sandwich plate was investigated when  $\mu=0.3$ ,  $\eta=1$ ,  $f_{r-max}=0.2$  and  $T=400$  K. Figure 9 shows that decreasing  $n$ , which indicated the increase of the amount of used CNT and accordingly improvement of the stiffness of resulted nanocomposite, increased the speeds and also decreased the amplitudes of wave propagations in sandwich plates.



**Figure 8.** Time histories of thermoelastic (a) deflection (b) normal stresses in nanocomposite sandwich plates with  $h/a=0.05$ ,  $h_f/h=0.1$ ,  $\eta=1$  and  $T=400$  K



**Figure 9.** Time histories of thermoelastic (a) deflection (b) normal stresses in nanocomposite sandwich plates with  $h/a=0.05$ ,  $h_f/h=0.1$ ,  $\mu=0.3$ ,  $\eta=1$ ,  $f_{r-max}=0.2$  and  $T=400$  K

Figure 10 compares the dynamic behaviors of plates with sandwich plates ( $h_f/h=0.1$ ) with the same thickness ( $h/a=0.05$ ) and CNTs volume fractions such that in sandwich plates  $f_r=0.2$  and in plates  $f_r=0.04$ . Furthermore, the effect of CNTs cluster states was explored by comparing the results obtained for  $\mu=1$  (fully dispersed CNTs) with those of  $\mu=0.3$  as shown in Figures 10a and 10b, respectively. In the case of  $\mu=1$ , Figure 10a shows that vibration amplitudes of

sandwich plates were much lower than plates which showed the successful performance of sandwich structures in damping vibrations. However, in case of  $\mu = 0.3$ , which meant the existence of CNT clusters, it was observed that the amplitude of vibrations in sandwich plates was higher than plates. The reason was the remarkable reduction of nanocomposite stiffness at higher  $f_r$  values due to the formation of CNT clusters.

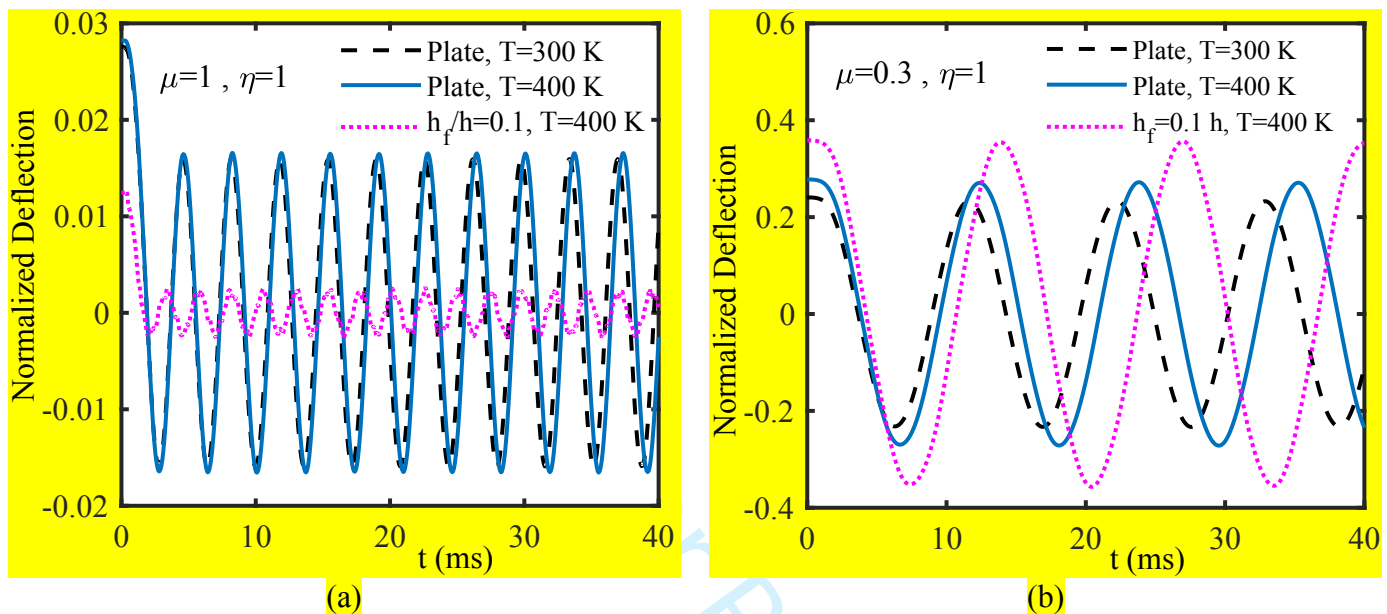


**Figure 10.** Comparison of central node vibrations of plates ( $f_r=0.04$ ) and sandwich plates ( $h_f/h=0.1$  and  $f_r=0.2$ ) with  $h/a=0.05, \eta=1$  and (a)  $\mu=1$  (b)  $\mu=0.3$

## 6. Conclusions

In this paper, after deriving the time histories of temperature from transient heat transfer problems, stress wave propagation in FG nanocomposite sandwich plates reinforced with CNT clusters were investigated using TSDT and a mesh-free method. The temperature-dependent material properties of nanocomposite were predicated by Eshelby-Mori-Tanaka's approach. The effects of CNT distribution, cluster size and volume fraction as well as thermal load on the thermoelastic dynamic behavior of the nanocomposite sandwich plates were examined. Our findings included:

- Temperatures at nanocomposite face sheets with lower  $n$  or higher CNT volume fractions were closer to their outer surface temperatures.
- Increasing CNT volume fraction reduced the required time for stationary condition.

- The effect of CNT distribution on the thermal behavior of nanocomposite plates were much higher than nanocomposite sandwich plates with the same thickness.
- The values of normal stresses were much higher than those of shear stresses in the sandwich plates subjected to thermo-mechanical loads.
- Increasing CNT volume fraction and/or cluster size reduced the amplitudes and increased the speeds of wave propagations.
- Rising environment temperature and/or increasing  $n$ , increase the amplitudes and reduce the speeds of wave propagations.
- The effect of CNT cluster size was much higher than CNT volume fraction on thermoelastic dynamic behavior.

## Acknowledgements

The work described in this paper was supported by Natural Science Foundation of China (51335006 and 11472148) and Natural Sciences and Engineering Research Council of Canada (NSERC under grant RGPIN-217525). The authors are grateful for their supports.

## References

- [1] Birmana V, Kardomateas GA. Review of current trends in research and applications of sandwich structures. *Compos Part B Eng* 2018;142:221–40.
- [2] Huang Z, Qin Z, Chu F. Vibration and damping characteristics of sandwich plates with viscoelastic core. *JVC/Journal Vib Control* 2016;22:1876–88. doi:10.1177/1077546314545527.
- [3] Huang Z, Qin Z, Chu F. A comparative study of finite element modeling techniques for dynamic analysis of elastic-viscoelastic-elastic sandwich structures. *J Sandw Struct Mater* 2016;18:531–51. doi:10.1177/1099636215623091.
- [4] Njuguna J. *Structural nanocomposites*. Springer; 2013.
- [5] Sofiyev AH, Hui D, Najafov AM, Turkaslan S, Dorofeyskaya N, Yuan GQ. Influences of shear stresses and rotary inertia on the vibration of functionally graded coated sandwich cylindrical shells resting on the Pasternak elastic foundation. *J Sandw Struct Mater* 2015;17:691–720. doi:10.1177/1099636215594560.
- [6] Iijima S. Synthesis of carbon nanotubes. *Nature* 1991;354:56–8.

- 1  
2  
3 [7] Lau K, Gu C, Hui D. A critical review on nanotube and nanotube/nanoclay related polymer  
4 composite materials. *Compos Part B* 2006;37:425–36.  
5  
6 [8] Kaushik BK, Majumder MK. Carbon nanotube based VLSI interconnects: Analysis and design.  
7 SpringerBriefs Appl. Sci. Technol., 2015, p. i–iv. doi:10.1007/978-81-322-2047-3.  
8  
9 [9] Safaei B, Naseradinmousavi P, Rahmani A. Development of an accurate molecular mechanics  
10 model for buckling behavior of multi-walled carbon nanotubes under axial compression. *J Mol*  
11 *Graph Model* 2016;65:43–60. doi:10.1016/j.jmngm.2016.02.001.  
12  
13 [10] Moradi-Dastjerdi R, Malek-Mohammadi H, Momeni-Khabisi H. Free vibration analysis of  
14 nanocomposite sandwich plates reinforced with CNT aggregates. *ZAMM - J Appl Math Mech*  
15 */ Zeitschrift Fur Angew Math Und Mech* 2017;97:1418–35. doi:10.1002/zamm.201600209.  
16  
17 [11] Moradi-Dastjerdi R, Malek-Mohammadi H. Biaxial buckling analysis of functionally graded  
18 nanocomposite sandwich plates reinforced by aggregated carbon nanotube using improved  
19 high-order theory. *J Sandw Struct Mater* 2017;19:736–69. doi:10.1177/1099636216643425.  
20  
21 [12] Alian AR, Kundalwal SI, Meguid SA. Multiscale modeling of carbon nanotube epoxy  
22 composites. *Polym (United Kingdom)* 2015;70:149–60. doi:10.1016/j.polymer.2015.06.004.  
23  
24 [13] Shokri-Oojghaz R, Moradi-Dastjerdi R, Mohammadi H, Behdinan K. Stress distributions in  
25 nanocomposite sandwich cylinders reinforced by aggregated carbon nanotube. *Polym Compos*  
26 2019;10.1002/pc.25206. doi:10.1002/pc.25206.  
27  
28 [14] Damadam M, Moheimani R, Dalir H. Bree's diagram of a functionally graded thick-walled  
29 cylinder under thermo-mechanical loading considering nonlinear kinematic hardening. *Case*  
30 *Stud Therm Eng* 2018;12:644–54. doi:10.1016/j.csite.2018.08.004.  
31  
32 [15] Kamarian S, Yas MH, Poursasghar A. Free vibration analysis of three-parameter functionally  
33 graded material sandwich plates resting on Pasternak foundations. *J Sandw Struct Mater*  
34 2013;15:292–308. doi:10.1177/1099636213487363.  
35  
36 [16] Shen H. Postbuckling of nanotube-reinforced composite cylindrical shells in thermal  
37 environments, Part I : Axially-loaded shells. *Compos Struct* 2011;93:2096–108.  
38 doi:10.1016/j.compstruct.2011.02.011.  
39  
40 [17] Ray MC, Kundalwal SI. A thermomechanical shear lag analysis of short fuzzy fiber reinforced  
41 composite containing wavy carbon nanotubes. *Eur J Mech A/Solids* 2014;44:41–60.  
42 doi:10.1016/j.euromechsol.2013.10.001.  
43  
44 [18] Zamani SMM, Iacobellis V, Behdinan K. Multiscale Modeling of the Nanodefets and  
45 Temperature Effect on the Mechanical Response of Sapphire. *J Am Ceram Soc* 2016;99:2458–  
46 66. doi:10.1111/jace.14243.  
47  
48 [19] Iacobellis V, Radhi A, Behdinan K. A bridging cell multiscale modeling of carbon nanotube-  
49 reinforced aluminum nanocomposites. *Compos Struct* 2018;202:406–12.  
50 doi:10.1016/j.compstruct.2018.02.044.  
51  
52 [20] Moheimani R, Hasansade M. A closed-form model for estimating the effective thermal  
53  
54  
55  
56  
57  
58  
59  
60

- 1  
2  
3 conductivities of carbon nanotube–polymer nanocomposites. *Proc Inst Mech Eng Part C J*  
4 *Mech Eng Sci* 2018;0:1–11. doi:10.1177/0954406218797967.
- 5  
6 [21] Safaei B, Fattahi AM, Chu F. Finite element study on elastic transition in platelet reinforced  
7 composites. *Microsyst Technol* 2018;24:2663–71. doi:10.1007/s00542-017-3651-y.
- 8  
9 [22] Safaei B, Fattahi AM. Free Vibrational Response of Single-Layered Graphene Sheets  
10 Embedded in an Elastic Matrix using Different Nonlocal Plate Models. *MECHANIKA*  
11 2017;23:678–87.
- 12  
13 [23] Zhang LW, Xiao LN. Mechanical behavior of laminated CNT-reinforced composite skew  
14 plates subjected to dynamic loading. *Compos Part B Eng* 2017;122:219–30.  
15 doi:10.1016/j.compositesb.2017.03.041.
- 16  
17 [24] Kolahchi R, Zarei MS, Hajmohammad MH, Nouri A. Wave propagation of embedded  
18 viscoelastic FG-CNT-reinforced sandwich plates integrated with sensor and actuator based on  
19 refined zigzag theory. *Int J Mech Sci* 2017;130:534–45. doi:10.1016/j.ijmecsci.2017.06.039.
- 20  
21 [25] Moradi-Dastjerdi R, Momeni-Khabisi H. Dynamic analysis of functionally graded  
22 nanocomposite plates reinforced by wavy carbon nanotube. *Steel Compos Struct* 2016;22:277–  
23 99. doi:http://dx.doi.org/10.12989/scs.2016.22.2.277.
- 24  
25 [26] Moradi-Dastjerdi R, Momeni-Khabisi H. Vibrational behavior of sandwich plates with  
26 functionally graded wavy carbon nanotube-reinforced face sheets resting on Pasternak elastic  
27 foundation. *J Vib Control* 2018;24:2327–43. doi:10.1177/1077546316686227.
- 28  
29 [27] Bisheh HK, Wu N. Analysis of wave propagation characteristics in piezoelectric cylindrical  
30 composite shells reinforced with carbon nanotubes. *Int J Mech Sci* 2018;145:200–20.  
31 doi:10.1016/j.ijmecsci.2018.07.002.
- 32  
33 [28] Bisheh HK, Wu N. Wave propagation characteristics in a piezoelectric coupled laminated  
34 composite cylindrical shell by considering transverse shear effects and rotary inertia. *Compos*  
35 *Struct* 2018;191:123–44. doi:10.1016/j.compstruct.2018.02.010.
- 36  
37 [29] Tornabene F, Fantuzzi N, Baccocchi M. Linear static response of nanocomposite plates and  
38 shells reinforced by agglomerated carbon nanotubes. *Compos Part B* 2017;115:449–76.
- 39  
40 [30] Qin Z, Yang Z, Zu J, Chu F. Free vibration analysis of rotating cylindrical shells coupled with  
41 moderately thick annular plates. *Int J Mech Sci* 2018;142–143:127–39.  
42 doi:10.1016/j.ijmecsci.2018.04.044.
- 43  
44 [31] Qin Z, Chu F, Zu J. Free vibrations of cylindrical shells with arbitrary boundary conditions : A  
45 comparison study. *Int J Mech Sci* 2017;133:91–9. doi:10.1016/j.ijmecsci.2017.08.012.
- 46  
47 [32] Setoodeh AR, Shojaee M. Application of TW-DQ method to nonlinear free vibration analysis  
48 of FG carbon nanotube-reinforced composite quadrilateral plates. *Thin-Walled Struct*  
49 2016;108:1–11.
- 50  
51 [33] Ghorbanpour Arani A, Jamali M, Mosayyebi M, Kolahchi R. Wave propagation in FG-CNT-  
52 reinforced piezoelectric composite micro plates using viscoelastic quasi-3D sinusoidal shear  
53  
54  
55  
56  
57  
58  
59  
60

- 1  
2  
3 deformation theory. *Compos Part B Eng* 2016;95:209–24.  
4  
5 doi:10.1016/j.compositesb.2016.03.077.
- 6 [34] Mohammadsalehi M, Zargar O, Baghani M. Study of non-uniform viscoelastic nanoplates  
7 vibration based on nonlocal first-order shear deformation theory. *Meccanica* 2017;52:1063–77.  
8  
9 doi:10.1007/s11012-016-0432-0.
- 10 [35] Sahmani S, Safaei B. Nonlinear free vibrations of bi-directional functionally graded  
11 micro/nano-beams including nonlocal stress and microstructural strain gradient size effects.  
12  
13 *Thin-Walled Struct* 2019;140:342–56. doi:10.1016/j.tws.2019.03.045.
- 14 [36] Alibeigloo A. Thermoelastic analysis of functionally graded carbon nanotube reinforced  
15  
16 composite cylindrical panel embedded in piezoelectric sensor and actuator layers. *Compos Part*  
17  
18 *B Eng* 2016;98:225–43. doi:10.1016/j.compositesb.2016.05.010.
- 19 [37] Mehar K, Panda SK, Dehengia A, Kar VR. Vibration analysis of functionally graded carbon  
20  
21 nanotube reinforced composite plate in thermal environment. *J Sandw Struct Mater*  
22  
23 2016;18:151–73. doi:10.1177/1099636215613324.
- 24 [38] Mehar K, Panda SK, Mahapatr TR. Thermoelastic nonlinear frequency analysis of CNT  
25  
26 reinforced functionally graded sandwich structure. *Eur J Mech - A/Solids* 2017;65:384–96.
- 27 [39] Asadi H. Numerical simulation of the fluid-solid interaction for CNT reinforced functionally  
28  
29 graded cylindrical shells in thermal environments. *Acta Astronaut* 2017;138:214–24.  
30  
31 doi:10.1016/j.actaastro.2017.05.039.
- 32 [40] Sobhaniragh B, Batra RC, Mansur WJ, Peters FC. Thermal response of ceramic matrix  
33  
34 nanocomposite cylindrical shells using Eshelby-Mori-Tanaka homogenization scheme.  
35  
36 *Compos Part B Eng* 2017;118:41–53. doi:10.1016/j.compositesb.2017.02.032.
- 37 [41] Thanh N Van, Khoa ND, Tuan ND, Tran P, Duc ND. Nonlinear dynamic response and  
38  
39 vibration of functionally graded carbon nanotube-reinforced composite (FG-CNTRC) shear  
40  
41 deformable plates with temperature-dependent material properties and surrounded on elastic  
42  
43 foundations. *J Therm Stress* 2017;40:1254–74. doi:10.1080/01495739.2017.1338928.
- 44 [42] Moradi-Dastjerdi R, Payganeh G. Thermoelastic dynamic analysis of wavy carbon nanotube  
45  
46 reinforced cylinders under thermal loads. *Steel Compos Struct* 2017;25:315–26.  
47  
48 doi:https://doi.org/10.12989/scs.2017.25.3.315.
- 49 [43] Moradi-Dastjerdi R, Payganeh G, Tajdari M. Thermoelastic Analysis of Functionally Graded  
50  
51 Cylinders Reinforced by Wavy CNT Using a Mesh-Free Method. *Polym Compos*  
52  
53 2018;39:2190–201. doi:10.1002/pc.24183.
- 54 [44] Fazzolari FA. Thermoelastic vibration and stability of temperature-dependent carbon nanotube-  
55  
56 reinforced composite plates. *Compos Struct* 2018;196:199–214.  
57  
58 doi:10.1016/j.compstruct.2018.04.026.
- 59 [45] Hosseini SM, Zhang C. Coupled thermoelastic analysis of an FG multilayer graphene platelets-  
60 reinforced nanocomposite cylinder using meshless GFD method: A modified micromechanical

- 1  
2  
3 model. *Eng Anal Bound Elem* 2018;88:80–92. doi:10.1016/j.enganabound.2017.12.010.
- 4 [46] Moradi-Dastjerdi R, Payganeh G. Transient heat transfer analysis of functionally graded CNT  
5 reinforced cylinders with various boundary conditions. *Steel Compos Struct* 2017;24:359–67.  
6 doi:https://doi.org/10.12989/scs.2017.24.3.359.
- 7  
8 [47] Lin H, Cao D, Shao C, Xu Y. Studies for aeroelastic characteristics and nonlinear response of  
9 FG-CNT reinforced composite panel considering the transient heat conduction. *Compos Struct*  
10 2018;188:470–82. doi:10.1016/j.compstruct.2018.01.028.
- 11  
12 [48] Pourasghar A, Chen Z. Hyperbolic heat conduction and thermoelastic solution of functionally  
13 graded CNT reinforced cylindrical panel subjected to heat pulse. *Int J Solids Struct*  
14 2019;163:117–29.
- 15  
16 [49] Pourasghar A, Chen Z. Effect of hyperbolic heat conduction on the linear and nonlinear  
17 vibration of CNT reinforced size-dependent functionally graded microbeams. *Int J Eng Sci*  
18 2019;137:57–72. doi:10.1016/j.ijengsci.2019.02.002.
- 19  
20 [50] Safaei B, Moradi-Dastjerdi R, Chu F. Effect of thermal gradient load on thermo-elastic  
21 vibrational behavior of sandwich plates reinforced by carbon nanotube agglomerations.  
22 *Compos Struct* 2018;192:28–37. doi:10.1016/j.compstruct.2018.02.022.
- 23  
24 [51] Safaei B, Moradi-Dastjerdi R, Qin Z, Chu F. Frequency-dependent forced vibration analysis of  
25 nanocomposite sandwich plate under thermo-mechanical loads. *Compos Part B Eng*  
26 2019;161:44–54. doi:10.1016/j.compositesb.2018.10.049.
- 27  
28 [52] Nan CW, Shi Z, Lin Y. A simple model for thermal conductivity of carbon nanotube-based  
29 composites. *Chem Phys Lett* 2003;375:666–9. doi:10.1016/S0009-2614(03)00956-4.
- 30  
31 [53] Shi D, Feng X, Huang YY, Hwang K-C, Gao H. The Effect of Nanotube Waviness and  
32 Agglomeration on the Elastic Property of Carbon Nanotube- Reinforced Composites. *J Eng*  
33 *Mater Technol* 2004;126:250–7. doi:10.1115/1.1751182.
- 34  
35 [54] Eshelby JD. The determination of the elastic field of an ellipsoidal inclusion, and related  
36 problems. *Proc R Soc London Ser A* 1957;241:376–96.
- 37  
38 [55] Mura T. *Micromechanics of Defects in Solids*, The Hague. Martinus Nijhoff Pub; 1982.
- 39  
40 [56] Reddy JN. *Mechanics of Laminated Composite Plates and Shells: Theory and Analysis*. CRC  
41 press; 2004.
- 42  
43 [57] Moradi-Dastjerdi R, Aghadavoudi F. Static analysis of functionally graded nanocomposite  
44 sandwich plates reinforced by defected CNT. *Compos Struct* 2018;200:839–48.  
45 doi:10.1016/j.compstruct.2018.05.122.
- 46  
47 [58] Song M, Kitipornchai S, Yang J. Free and forced vibrations of functionally graded polymer  
48 composite plates reinforced with graphene nanoplatelets. *Compos Struct* 2017;159:579–88.  
49 doi:10.1016/j.compstruct.2016.09.070.
- 50  
51  
52  
53  
54  
55  
56  
57  
58  
59  
60

**RESPONSES TO REVIEWERS****Ms. Ref. No.: JSSM-18-0331****Determination of thermoelastic stress wave propagation in  
nanocomposite sandwich plates reinforced by clusters of CNTs****B. Safaei, R. Moradi-Dastjerdi, Z. Qin, K. Behdinan, F. Chu**

Dear Editor,

We wish to thank you for the timely processing of our article in “Journal of Sandwich Structures & Materials” and the reviewers for their constructive comments, which have helped us clarify a number of issues in our manuscript. We have attended to all raised points/concerns in this revised manuscript. Given below are our responses and the suggested revisions to the article, as highlighted in the manuscript.

Sincerely yours,

Fulei Chu  
PhD (Southampton)  
Professor of Mechanical Engineering  
Tsinghua University  
Dated: April 13, 2019

## RESPONSES TO REVIEWER #1:

Dear Editor and Authors,

I have just completed my report in a detailed manner. As a general evaluation result in reviewing, in recent years, the applications of finite element method to the differential equations are of an increasing interest in different application areas. In this sense, from the mathematical point of views, this work takes play an important role in this field. The authors investigate some important properties for the model considered. The results are almost satisfactory. However, there are some grammatical corrections. After corrections, this paper should be accepted for publishing in the journal.

Briefly, I think that this interesting paper will contribute to the journal when it is published. I recommend to publish this paper after polish in English.

With my best regards

### Response:

We wish to thank the reviewer for taking his/her time to review the paper. The revised version has been carefully modified in terms of writing.

## RESPONSES TO REVIEWER #2:

The authors are very grateful to the reviewer for his/her careful review of the manuscript, insightful comments, and recommendations to help paper be accepted in the journal. We have considered and attended to all the raised points/concerns. Given below is our responses and suggested revisions to the article.

### Comments to the Author:

1. Too lengthy introduction part needs to be revised.

#### Response:

We wish to thank the reviewer for this comment. The entire of “introduction” section has been modified in the revised version of the manuscript.

2. Few references are not adding information to the manuscript, may be revise the references

**Response:**

The mentioned references have been removed or replaced as highlighted in the manuscript.

3. The mechanical behavior of the composite face sheets already studied by the authors may be included in this manuscript to know the deviation of the performances after the addition of CNT clusters.

**Response:**

According to the employed Eshelby–Mori–Tanaka’s approach, there are three types of nanocomposites: those are reinforced with (i) aligned CNTs (ii) randomly oriented CNTs and (iii) clusters of randomly oriented CNTs. Note that the second type is a specific type of third one ( $\mu=\eta$ ). In this paper, we have studied the effects of the formation on CNT clusters on the dynamic behaviors of nanocomposites. Therefore, we only included the required equations for estimated of the mechanical properties of polymer/CNT cluster. Please see Eqs. 3-11.

**RESPONSES TO REVIEWER #3:**

The authors would like to thank the reviewer for his/her constructive comments which helped us to improve the quality of the article. We have attended to the raised points/concerns and we trust that the paper is now suitable for publication. Given below is a summary of our responses and suggested revisions to the article.

**Comments to the Author:**

Transient heat transfer and stress wave propagation in polymeric sandwich plates with two nanocomposite face sheets with FG volume fractions of CNTs and their clusters along the thickness of face sheets were investigated for thermo-mechanical loading conditions. Eshelby-Mori-Tanaka’s approach was applied to evaluate the material properties of the resulted nanocomposite with components with temperature-dependent material properties. The third order shear deformation theory (TSDT) is used for modeling the mechanical behavior of sandwich plate and the meshless method is employed for solution of the problem and the effects of CNT cluster parameters and loading on the thermoelastic dynamic behavior of nanocomposite sandwich plates were investigated.

The topic is interesting. The following comments and questions must be implied or answered.

- 1  
2  
3 1. The literature review must be improved and focused on the topic, so that it shows the novelty  
4 and state-of-art of the present paper. It is only a simple list of papers in the field of FG-CNTRC  
5 plates and shells.  
6

7 **Response:**

8 Thank you for pointing out this direction. The entire of “Introduction” section has been  
9 modified.  
10  
11  
12

- 13  
14 2. The English writing of the paper needs some improvements, for example Page 4 line36 “face  
15 sheets subjected to thermal gradient loads were and evaluated [55,56].”  
16

17 **Response:**

18 The revised manuscript has been carefully modified in terms of writing.  
19  
20  
21  
22

- 23  
24 3. The node distribution of the meshless discretization is not presented in the manuscript.  
25

26 **Response:**

27 In the presented dynamic analyses of sandwich plates,  $15 \times 15$  node arrangement and  $14 \times 14$   
28 background cells with 4 Gauss points in each cell for the integration of local mass and stiffness  
29 matrices has been adopted.  
30

31 This point was added to the revised manuscript. Please see page 14.  
32  
33  
34  
35

- 36 4. The convergence study of the results for the number of nodes is not studied. The dependency  
37 of results to number of nodes must be studied.  
38

39 **Response:**

40 We changed Fig. 3 to show the convergence of the developed method. In the new figure, it  
41 was observed that increasing the number of nodes in each direction from 5 to 17 led to more  
42 accurate dynamic results such that the use of  $17 \times 17$  node arrangement provided a very good  
43 agreement with results reported in literature. In addition, the increase of node numbers from  
44 9 to 17 had an insignificant effect on the accuracy of results. Please see the description of Fig.  
45 3 in page 13.  
46  
47  
48  
49  
50

- 51 5. The results of meshless methods depend on the solution parameters such as the size of  
52 subdomains, support domains. There is no information about the meshless discretization of  
53 the problem.  
54

55 **Response:**

1  
2  
3 As mentioned in the response of third comment, we have utilized 15×15 node arrangement  
4 and 14×14 background cells with 4 Gauss points in each cell for the integration of local mass  
5 and stiffness matrices has been adopted.  
6

7 This point was added to the revised manuscript. Please see page 14.  
8  
9

- 10  
11 6. Which method is used for time integration of the discretized equations? Please explain more  
12 about the method and the chosen time step  $\Delta t$ .  
13

14 **Response:**

15  
16 We utilized Newmark (central difference) method for the solution of the discretized equations  
17 (Eq. 29). In this method, time step  $\Delta t$  must be lower than the critical value which is equal to  
18  $\Delta t \leq \Delta t_{cr} = (\omega_{max}^2 / 4)^{-1/2}$ . Here  $\omega_{max}$  is the maximum value of natural frequencies. Meanwhile,  
19 the accuracy of the utilized Newmark (central difference) method is in the order of  $\Delta t^2$ . We  
20 added the use of this method in the revised manuscript. Please see page 10.  
21  
22

- 23  
24  
25 7. It seems that the third equation of (1) must be written as  $f_r = (1 - (2z+h)/(2hf))^n f(r_{max})$   
26

27 **Response:**

28 Thank you for pointing out this mistake. We have corrected it in the revised manuscript.  
29  
30

- 31  
32  
33 8. According to equation 1,  $f_r(h/2-hf) = f_r(-h/2+hf) = 0$ , although this distribution has not problem,  
34 but it is not general and limited volume fraction of one side of the interface to zero.  
35

36 **Response:**

37 We wish to thank the reviewer for raising this point. We proposed Eq. 1 to show a continuous  
38 variation of material properties from neat polymeric core to FG nanocomposite face sheets.  
39 Moreover, in sandwich plates with UD nanocomposite face sheets, CNT volume fractions at  
40 inner faces are not zero.  
41  
42

43 The justification of proposing Eq. 1 has been added to the article. Please see pages 4-5.  
44  
45

- 46  
47 9. The presented numerical results are not sufficient and more figures tables can be added to the  
48 numerical results to show the impact of the work and give deep sense about the physical  
49 behavior of plate.  
50

51 **Response:**

52 Thank you for this point. By adding Figs. 10a and 10b, we also investigated the effects of  
53 CNT cluster formation on the dynamic behavior of the proposed structures as well as the  
54  
55  
56  
57  
58  
59

1  
2  
3 differences between the dynamic behavior of plates and sandwich plates. Please see pages 18-  
4 19.  
5  
6  
7

- 8 10. What is the nature of fluctuations in the results? Please interpret the fluctuations. Do the  
9 fluctuations have physical nature or they are numerical fluctuations.  
10

11 **Response:**

12 The authors thank the reviewer for raising this important point.

13  
14 As shown in Figs. 7-9, fluctuations were only appeared in the time histories of in-plane  
15 stresses of sandwich plates which were under both mechanical and thermal loads. The most  
16 important reason could be the constant values of thermal strain (Eq. 17) in all cycles. However,  
17 numerical issues could be another reason for these fluctuations.  
18  
19  
20  
21  
22  
23

24 The authors wish to reiterate their gratitude to the reviewers for their insightful comments and  
25 taking time to carefully review our work. We feel that they have helped us improve the quality and  
26 content of our manuscript.  
27  
28  
29

30 Sincerely yours,

31  
32 Fulei Chu  
33 PhD (Southampton)  
34 Professor of Mechanical Engineering  
35 Tsinghua University  
36  
37  
38  
39  
40  
41  
42  
43  
44  
45  
46  
47  
48  
49  
50  
51  
52  
53  
54  
55  
56  
57  
58  
59  
60